Wu *et al.*
Journal of Analytical Science and Technology (2024) 15:40
https://doi.org/10.1186/s40543-024-00454-0

Journal of Analytical Science and Technology

RESEARCH ARTICLE Open Access

Exonuclease III assisted exponential amplification reaction (EXPAR) for specific miRNA-155 analysis during post-anesthetic nursing

Xuejun Wu[1†], Shaolan Zou[1†] and Jingshen Dai[1*]

Abstract

The persistent obstacle in precise and sensitive identification of microRNAs (miRNAs) pertains to the advancement of expeditious and effective isothermal amplification methodologies suitable for point-of-care environments and monitoring the cancer prognosis in patients receiving post-anesthetic nursing. The exponential amplification reaction (EXPAR) has attracted considerable interest due to its simplicity and ability to rapidly amplify signals. The practical application of the EXPAR is, nevertheless, severely hampered by the inability to differentiate closely related homologous sequences and to modify the designed templates to suit other targets. A loop-stem template for the EXPAR system was developed in this study to facilitate specific target recognition with the aid of exonuclease III (Exo III). This innovation effectively eliminated non-specific hybridization that could occur between the template and interfering sequences, thereby ensuring minimal background amplification of EXPAR. By modulating Exo III-based target recycling, EXPAR based chain amplification and G4/hemin based color reaction, this method facilitated the precise and sensitive examination of miRNA-155, yielding acceptable yields and a minimal detection limit of 0.43 fM. The approach expedites simple and expeditious molecular diagnostic applications involving short nucleic acids and offers an innovative method for enhancing the selectivity of EXPAR-based techniques, providing a robust tool for monitoring the expression level from patients receiving post-anesthetic nursing and guiding the treatment strategy.

Keywords Exponential amplification reaction (EXPAR), Exonuclease III (Exo III), microRNAs (miRNAs), Colorimetric assay

Introduction

MicroRNAs (miRNAs), which originate from endogenous hairpin transcripts, belong to a category of brief, non-coding RNAs with a single strand (Saliminejad et al. 2019; Rupaimoole and Slack 2017). Their function is to control gene expression through posttranscriptional mechanisms, specifically by promoting mRNA cleavage or translational repression (Ho et al. 2022; Mishra et al. 2016; Parayath et al. 2022). An expanding body of research indicates that aberrant miRNA expression is intricately linked to the development, progression, and metastasis of various diseases, especially cancer (He et al. 2020; Hussen et al. 2021). For example, miRNA-155 has been recognized as a novel biomarker for assessing clinical progression of hepatocellular carcinoma and postoperative tumor recovery (Ratnasari et al. 2022). Furthermore, the aberrant expression of miRNA level serves as a crucial reference point for

†Xuejun Wu and Shaolan Zou have contributed equally to this work.

*Correspondence:
Jingshen Dai
Hzy123456782024@163.com
[1] Department of Anesthesiology, People's Hospital of Chongqing, Liang Jiang New Area, No. 199, Renxing Road, Chongqing 401121, China

assessing anesthesia status and adjusting postoperative nursing strategy (Yang et al. 2016; Bai et al. 2022). Nevertheless, the intrinsic qualities of miRNAs, including their low abundance, small size, and high degree of sequence homogeneity with other members of the family, have presented difficulties in achieving convenient, sensitive, and precise multiplex detection.

The conventional techniques employed for the identification of miRNAs consist of RNA sequencing, quantitative real-time PCR (qRT-PCR) (Chen et al. 2005; Forero et al. 2019; Takei et al. 2020), and microarrays (Li et al. 2009). While these techniques facilitate the detection of miRNAs on multiple occasions, they may entail intricate, costly, and time-consuming procedures. Furthermore, as a standard method for quantifying microRNAs, qRT-PCR is extremely sensitive to fluctuations in temperature and the judicious selection of primers and probes; furthermore, its ability to multiplex is limited by the number of available fluorescence channels. For the sensitive detection of miRNAs, numerous signal amplification strategies have been devised in recent years, including rolling circle amplification (Xu et al. 2021; Zhao et al. 2008), catalytic hairpin assembly (Zhao et al. 2021; Wu et al. 2021), and exponential amplification reaction (EXPAR) (Wei et al. 2022; Reid et al. 2018). EXPAR is one of these techniques that offers exceptional kinetics, low cost, and a high degree of sensitivity (10^6–10^9 fold) oligonucleotide amplification in less than 30 min under isothermal conditions (Emaus and Anderson 2021; Chen et al. 2021; Guo et al. 2024). As an illustration, Jia et al. devised an exceptionally sensitive technique by employing real-time fluorescence detection to identify the EXPAR products generated in response to miRNAs (Jia et al. 2010). The significant background amplification that EXPAR encounters is a primary obstacle that restricts its practical implementation. Similar sequences whose 3' terminus is complementary to the template have the potential to initiate EXPAR. This increases the possibility of non-specific amplification and makes non-specific amplification more difficult to control, owing to the extremely high amplification efficiency. As a result, there is an imperative need for the development of EXPAR-based miRNA detection methods with significantly increased specificity and minimal background signals.

The exonuclease amplification reaction, which utilizes exonuclease III (Exo III), has garnered considerable attention due to its economical nature and exceptional shear efficiency (Guo et al. 2023; Hu et al. 2023). The sequential elimination of individual nucleotides from the blunt or recessed 3-OH termini of dsDNA is catalyzed by Exo III, irrespective of the targeting nucleic acid sequences. By increasing the selectivity of the complementary sequences in dsDNA, Exo III guarantees a high degree of specificity.

To detect miRNA-155, we developed in this article a colorimetric sensor with significantly enhanced selectivity and sensitivity by utilizing Exo III-assisted target recycling and EXPAR-assisted signal amplification. The template in EXPAR is exposed for subsequent high-efficiency signal amplification following target recognition by Exo III and cleavage of the complementary sequences; this eliminates the possibility of non-specific initiation of EXPAR by a similar sequence. The sensor demonstrates an exceptionally high sensitivity in detecting miRNA-155 and an exceptionally high selectivity towards sequences that involve even a single base mismatch.

Experimental section

Materials and reagents

All the sequences used for the construction of the method were custom-synthesized by Sangon Biotechnology Co., Ltd. (Shanghai, China), and the details of oligonucleotides were shown in Table S1. Essential enzymes for the signal amplification process, including Exo III, Klenow fragment polymerase, Nt.BsmAI, and 10×NEBuffer 2 (50 mM of NaCl, 10 mM of Tris–HCl, 10 mM of $MgCl_2$, and 1 mM dithiothreitol, pH 7.9) were obtained from New England Biolabs (USA). Yuanye Bio-Technology Co., Ltd (Shanghai, China) supplied the hemin and Sangon Biotech Co., Ltd (Shanghai, China) provided ABTS. UV–vis absorption was detected by using a Hitachi U-4100 UV–vis spectrophotometer (Kyoto, Japan).

Preparation of the LT probe system

The LT probe dilisted (20 μM) in 20 mM Tris–HCl buffer (pH 7.8, 40 mM KCl, 8 mM $MgCl_2$, and 0.05% Triton X-100) was firstly heated to 90 °C for 10 min, and then the solution was cooled to 37 °C for 20 min for hybridization of stem-loop structure. The assembled LT probe was stored at 4 °C before further application.

Detection procedures of the method

Exonuclease III assisted enzyme amplification reaction

Duirng the Exo III assisted amplification reaction, 2μL of LT probe (100 nM), different concentrations of miRNA-155, and 2μL of Exo III (0.2 U/μL) were incubated separately in Tris buffer for 30 min at 37 °C. Afterwards, the solution was heated to 70 °C for 15 min to inactivate Exo III enzyme.

For the EXPAR pecrdure

Two reaction solutions were prepared for the EXPAR reaction (components A and B). In detail, the solution A is composed of Nt.BstNBI buffer, the above solution,

dNTPs, primer sequences (100 nM), and RNase inhibitor. The solution B is composed of DEPC-treated water, 5 μL of ThermoPol buffer, 2 μL of Nt.BstNBI (0.2 U/μL), and 2 μL of DNA polymerase (0.03 U/μL). After the preparation of the two solutions, solutions A and B were mixed immediately on ice with a final volume of 50 μL.

Color reaction

For the color reaction, 5 μL of the prepared hemin (400 nM) was added to the reaction solution. The solution was further incubated at 37 °C for 30 min. Finally, both 2 μL of H_2O_2 (1 mM) and 5 μL of ABTS (1 mM) were mixed with the above reaction solutions, and the absorbance levels were recorded at 418 nm.

Results and discussion

The working mechanism of the proposed EXPAR-based sensor for miRNA detection

The diagram in Fig. 1 illustrates the detection principle of miRNA-155 utilizing the proposed colorimetric sensor. The detection procedure is divided into three stages: (1) an enzymatic amplification reaction utilizing Exo III in solution; (2) EXPAR system designed to efficiently produce "4" chains; and (3) a color reaction based on ABTS. This approach involves the development of a loop-stem LT probe that incorporates EXPAR for signal amplification and Exo III-assisted target recognition. (1) When miRNA-155 is present, the stem-loop segment of the LT probe, which possesses exposed base sequences at its 3' extremities, can produce a flat end with miRNA-155 that can be specifically recognized by Exo III. The successive Exo III-based hydrolysis of "1" and "2" in LT probe resulted in the TS (template for EXPAR), and release of miRNA-155 from the miRNA/LT duplex. The released miRNA-155 continues the enzymatic digestion cycle, forming the Exo III assisted signal cycle. The reaction is terminated by heating the solution to 70 °C for 10 min. (2) TS includes two similar sequences ("3" and "3*") and a sequence complementary to the restriction endonuclease Nt.BstNBI recognition site in the middle. The amplification cycle, which is coordinated with template 3-5-3*,

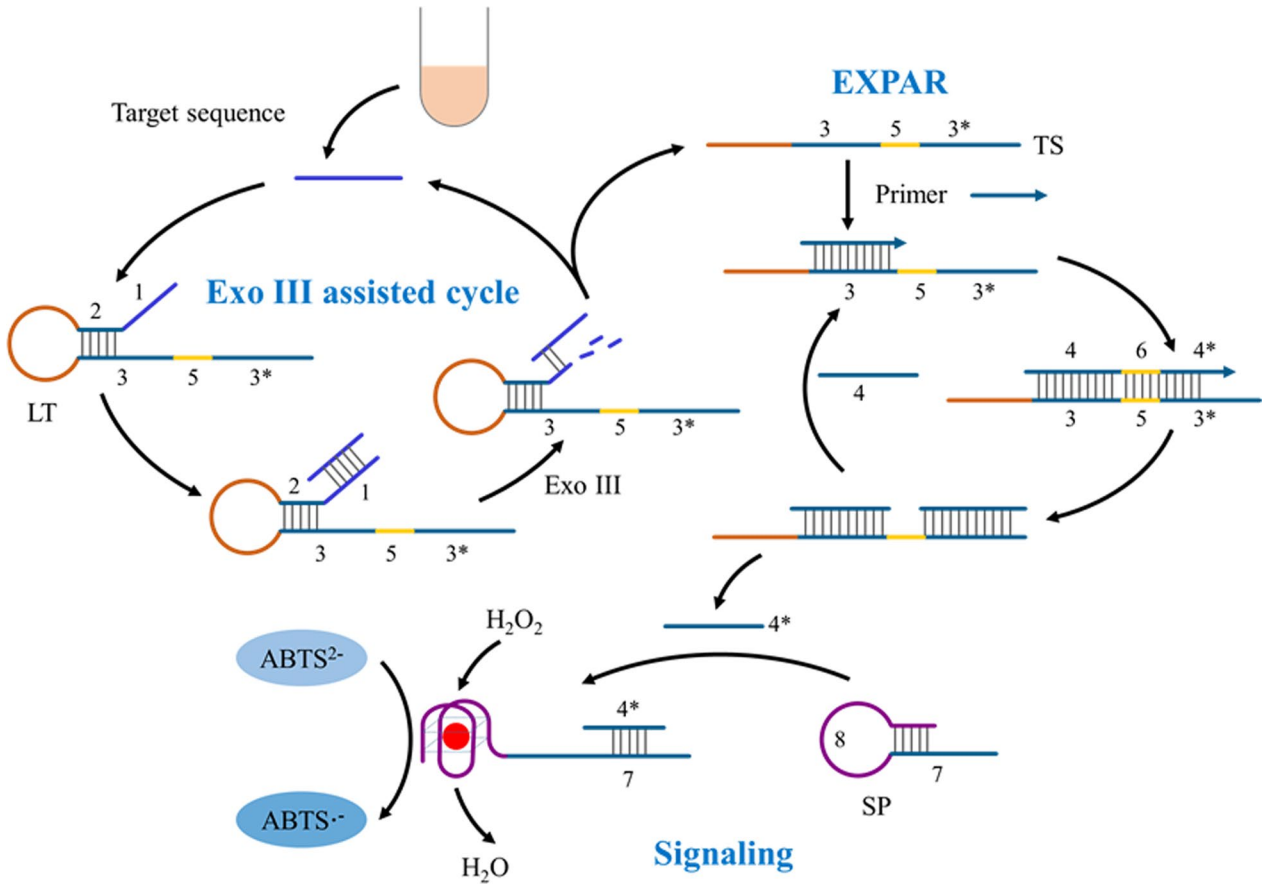

Fig. 1 The principle of the established EXPAR-based colorimetric method, including the Exo III assisted cycle, EXPAR process, and the signaling process

is initiated when the "Primer" is present. The dsDNA products containing a nicking enzyme recognition site on the top strand are generated when the DNA polymerase catalyzes the extension of the "Primer" nucleic acid. The nicking endonuclease cleaves the top strand, releasing the newly generated specific amplicon "4*" from the TS. In order to generate a substantial quantity of "4*," the newly produced "4*" can bond with another TS to initiate additional amplification cycles involving duplex extension, nicking, and release. (3) The disassociation of the SP probe by the "4*" chains liberate the G-rich segment that can fold into G-quadruplexes. By utilizing HRP-mimicking G-quadruplex/hemin complexes to catalyze ABTS into $ABTS^{\cdot+}$, it is possible to conduct colorimetric analysis of miRNA-155 through UV–vis spectrophotometry or by naked eyes.

Feasibility of the colorimetric sensor for miRNA-155 analysis

Fluorescent examination was conducted using SYBR Green I to verify the practicality of the Exo III-aided signal cycle. SYBR Green I can analyze the production of double-stranded DNA segments in the LT probe, such as the stem section, and provide fluorescence signals. Figure 2A demonstrates that the SYBR Green I signal in the system is minimal prior to the assembly of LT into a stem-loop structure (column 1). Upon heating the LT probe to 90 °C and thereafter cooling it gradually to room

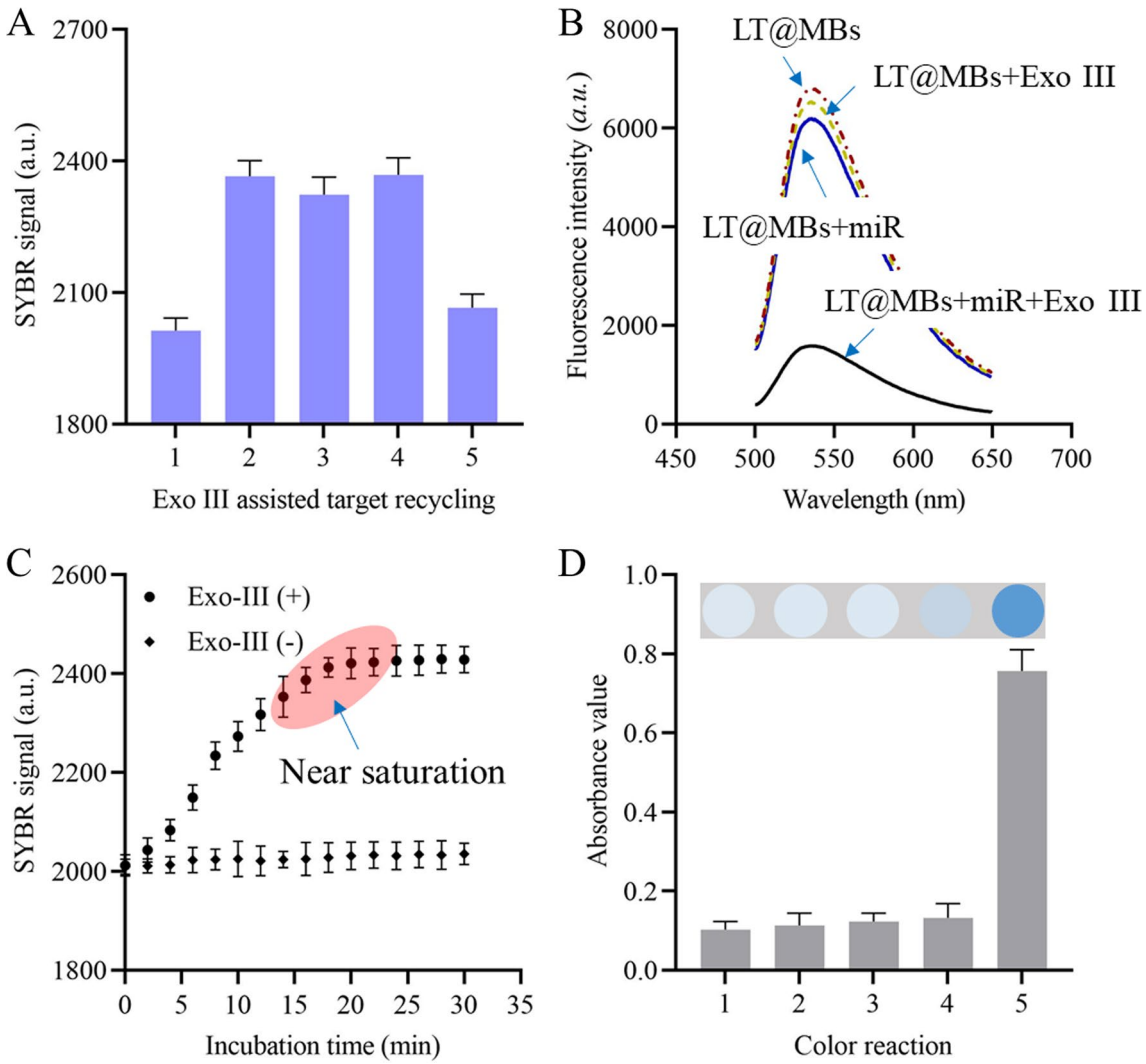

Fig. 2 Feasibility analysis of the sensor. **A** SYBR Green I signals of the LT probe during the Exo III assisted target recycling process. **B** Fluorescence spectrum of the FAM labeled LT probe during the Exo III assisted target recycling process. **C** SYBR Green I signals during the EXPAR process. **D** Absorbance values of the color reaction when hemin, target, and Exo III existed or not. Data were expressed as mean ± standard deviations, n = 3 technical replicates

temperature, the SYBR Green I signal exhibited a notable increase, suggesting the creation of double-stranded DNA structure and confirming the successful assembly of the stem-loop structure (column 2). Exo III's presence did not result in a significant rise in the SYBR Green I signal, indicating that the stem structure remained intact (column 3). Upon the introduction of miRNA-155 into the system, a notable reduction in the SYBR Green I signal was detected, indicating that the stem was cleaved by Exo III (column 5). On the contrary, the SYBR Green I signal remained in high level, when the miRNA-155 was incubated with the LT probe, implying the Exo III was crucial for the feasibility of the Exo III assisted target recycling.

In order to provide additional evidence that Exo III cleaves the "1" and "2" components, the 3′-end of LT is marked with the fluorescent dye FAM, while the 5′-end is labeled with avidin and attached to the magnetic bead by an interaction with streptavidin. The fluorescence signals on the surface of magnetic beads were recorded and compared after performing magnetic enrichment and removing the supernatant. When LT was combined with Exo III and miRNA-155, the fluorescence signal on the magnetic beads' surface was considerably diminished, indicating that the "1" and "2" components underwent hydrolysis. In contrast, the absence of Exo III or miRNA-155 did not result in any notable difference between the fluorescence signal detected on the magnetic bead surface and that of the control group (Fig. 2B).

Real-time fluorescence monitoring was subsequently utilized to verify the EXPAR process. A time-dependent increase in the fluorescence of SYBR Green I is evident, as illustrated in Fig. 2C. The SYBR Green I signals ceased to increase after the EXPAR was carried out for over 20 min, suggesting that the condition had become saturated and all TS sequences were occupied by the generated "4*" chains. Without the Exo-III, no significant elevation of SYBR Green I signal could be observed, indicating that the EXPAR process could not be initiated with the Exo-III.

To investigate the strategic feasibility, the ABTS–H_2O_2 system was used to study the prepared probe system (column 1). As depicted in Fig. 2D, the absorbance of hemin at 418 nm was significantly reduced (column 2) when it was the only component in the system solution. Consequently, the solution appeared colorless because hemin had minimal catalytic activity in the ABTS–H_2O_2 system. Upon the introduction of both target and hemin into the ABTS-H_2O_2 solution, a notable rise in absorbance at 418 nm was detected, accompanied by a dark green coloration of the solution. This can be attributed to the binding of hemin with a G-quadruplex, resulting in the formation of the HRP-mimicking DNAzyme of the G-quadruplex/hemin conjugate (column 5). Nevertheless, in the absence of Exo III, the solution lacked color and its absorbance at 418 nm remained low due to the absence of free G-quadruplexes that might bind with hemin to produce the conjugate (column 4).

Optimization of experimental conditions

In order to achieve the best performance of the EXPAR analytical method, we optimized the experimental conditions, which involved optimizing the reaction time and the concentrations of polymerase and Nt.BsmAI. The exponential nature of EXPAR made it prone to non-specific amplification. In this study, we utilized the signal-to-noise (S/N) ratio as a metric to evaluate the performance of the system. Initially, the reaction time was assessed. According to the data presented in Fig. 3A, the fluorescence signal experienced a significant increase between 10 and 30 min. It then reached a plateau before the 30 min, indicating the exponential amplification of EXPAR. However, the S/N ratio gradually fell after 30 min, as the background signal became stronger. Thus, a reaction time of 30 min was selected as the most favorable in the subsequent studies. Figure 3B displays the absorbance signal at different doses of Nt.BsmAI. The highest S/N ratio was recorded at an enzyme concentration of 1.5 U/μL Nt.BsmAI, indicating that the level of non-specific amplification was minimized. In addition, Fig. 3C demonstrates that the augmentation of polymerase concentration led to a corresponding rise in absorbance, reaching its peak at a concentration of 0.2 U /μL. Increasing the dosage of polymerase would elevate the background, leading to a decrease in the S/N ratio of the EXPAR-based method. Thus, the most effective concentration of polymerase was determined to be 0.2 U/μL. The ideal concentration of Exo III was determined to be 0.2 U/μL, which aligns with the concentration reported in the literature (Fig. 3D).

Analytical performance of the proposed method

Figure 4A, B display the absorbance responses of the sensor at various concentrations of miRNA-155, under optimal reaction circumstances, to assess the sensor's sensitivity. As the concentration of miRNA-155 climbed from 1 fM to 100 pM, there was a progressive increase in the absorbance value peak. The peak value and logarithm of the target miRNA-155 concentration were compared. A strong linear correlation was seen between the peak value and the target miRNA-155 concentration, spanning a range of 1 fM to 1 nM. The linear regression equation, $A_{target} = 0.1179*lgC + 0.2455$ ($R^2 = 0.996$), was derived. The detection limit, determined using the 3σ approach, was found to be 0.43 fM, which is exceptionally low. Our sensor exhibits superior performance in terms of a lower

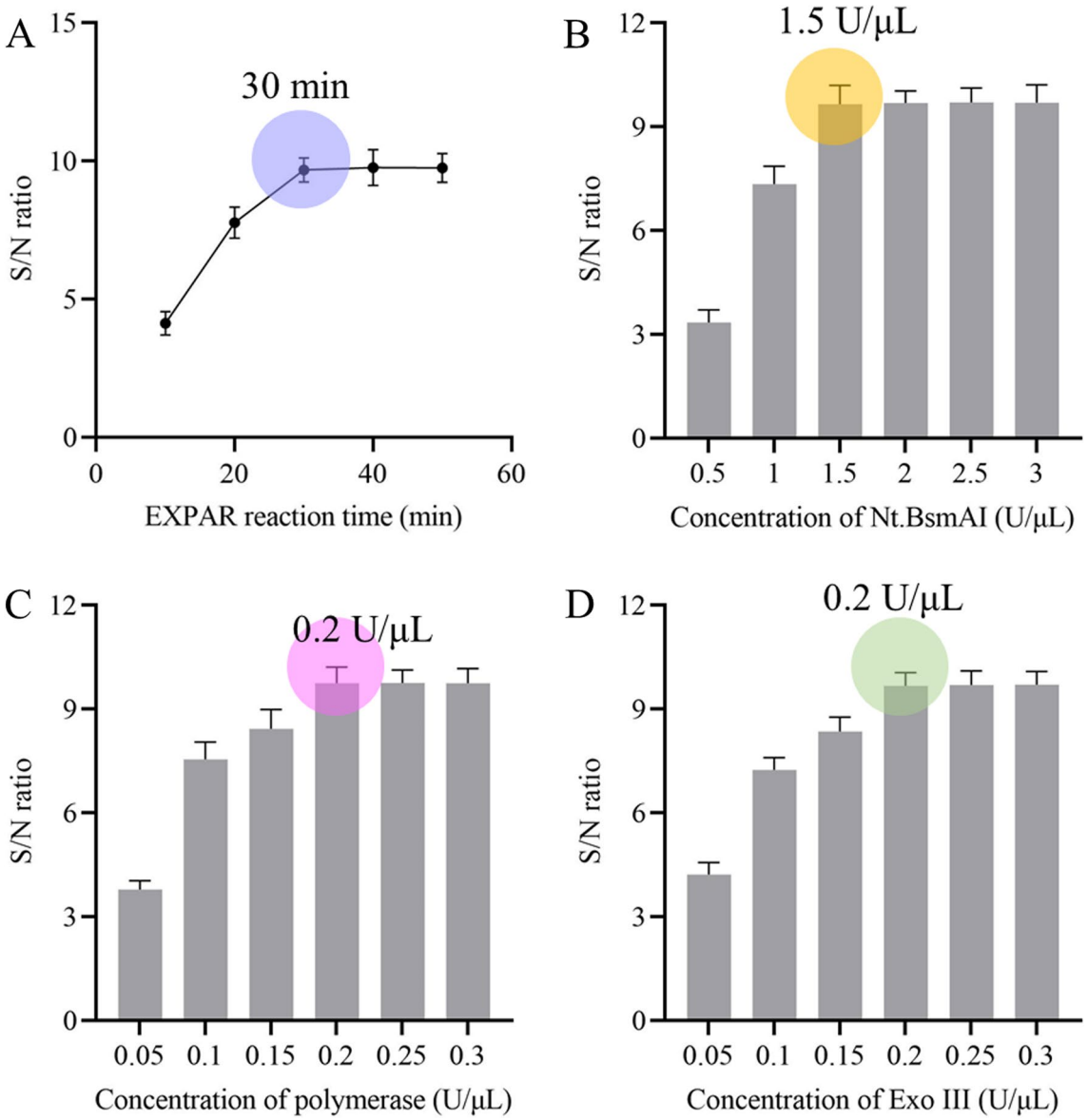

Fig. 3 Optimization of experimental parameters. The signal-to-noise (S/N) of the sensor when detecting miRNA with different incubation time (**A**), and different concentration of Nt.BsmAI (**B**), polymerase (**C**), and Exo III (**D**). Data were expressed as mean ± standard deviations, n = 3 technical replicates

detection limit and a larger linear range when compared to conventional detection methods (Table S2).

In order to determine the specificity of the suggested sensor, we conducted a comparison of the absorbance response of miRNA-155 (10 pM) with other microRNAs (10 pM), such as microRNA-141 (miR-141), microRNA-21 (miR-21), single-base mismatched miRNA-155 (smiR-155), and triple base mismatched miRNA-155 (tmiR-155). These were evaluated using identical experimental parameters. According to Fig. 4C, the absorbance values of the detection targets were not statistically different from the blank samples, except for miRNA-155. However, the signal peaks of miRNA-155 were significantly greater. These results demonstrate that the proposed biosensor has high specificity in detecting miRNA-155.

Application potential of the method for miRNA-155 detection

In order to assess the reproducibility of the sensor, six duplicate samples containing miRNA-155 (10 pM) were analyzed using the optimized reaction conditions. The

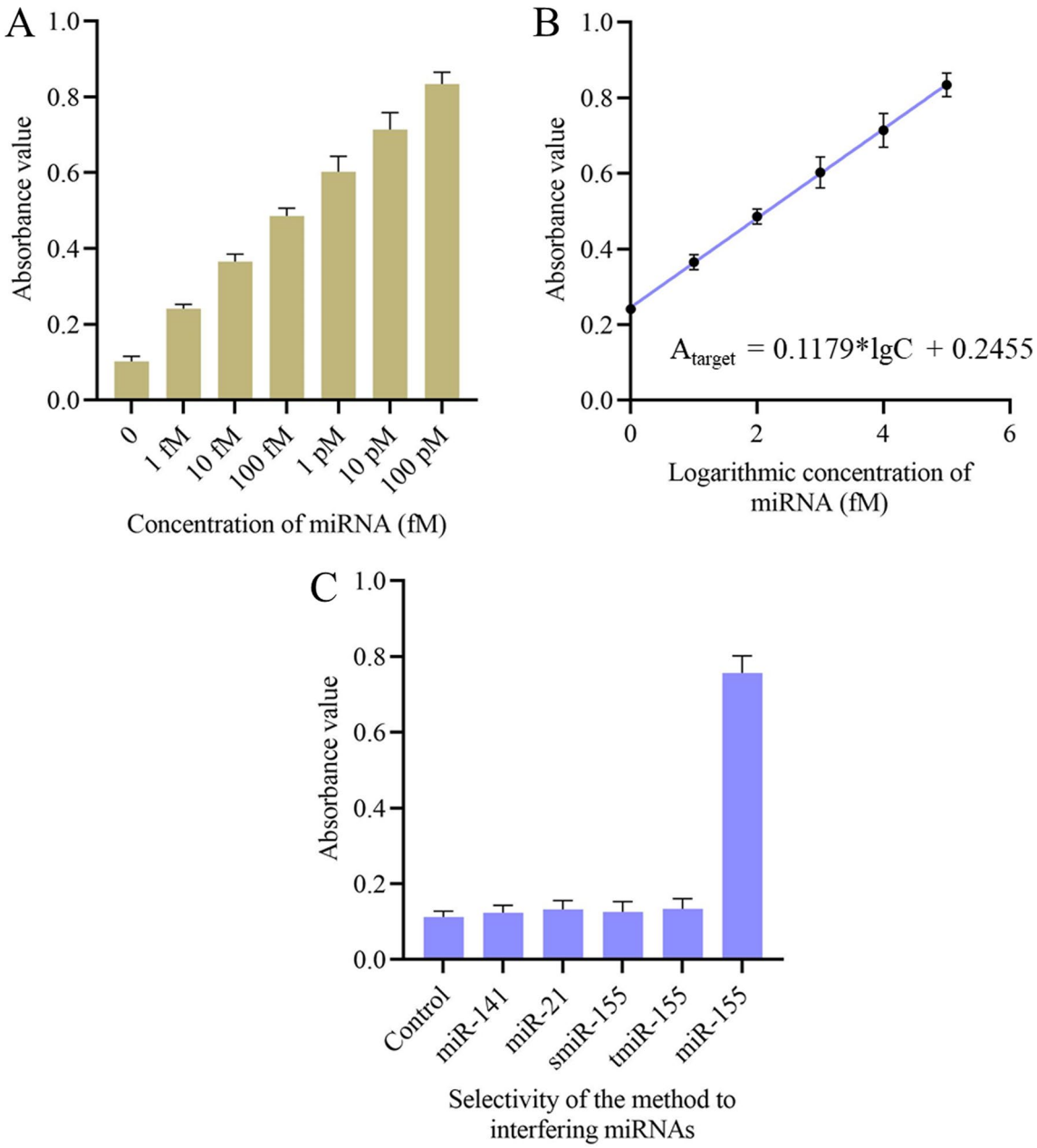

Fig. 4 Analytical performance of the sensor. **A** Absorbance value of the method when detecting different concentrations of miRNA. **B** Correlation between the absorbance value of the method and concentrations of miRNA. **C** The absorbance value of the method when detecting interfering miRNAs. Data were expressed as mean ± standard deviations, n = 3 technical replicates

obtained absorbance values showed a relative standard deviation (RSD) of 3.43%, indicating that the sensor exhibited excellent reproducibility (Fig. 5A).

Testing the stability of the sensor is another parameter that needs to be evaluated. The sensor that was created was kept in a refrigerator at a temperature of 4 °C for a duration of one week. During this time, the average absorbance value was found to be 92.31% of the original average value, with an RSD of 3.96% based on a sample size of 5. This indicates that the sensor exhibited good stability, as shown in Fig. 5B.

Furthermore, the practical use of the biosensor was assessed using real samples acquired from cancer patients receiving postoperative care. The recovery studies involved the addition of varying quantities of miRNA-155 to serum, followed by detection using the

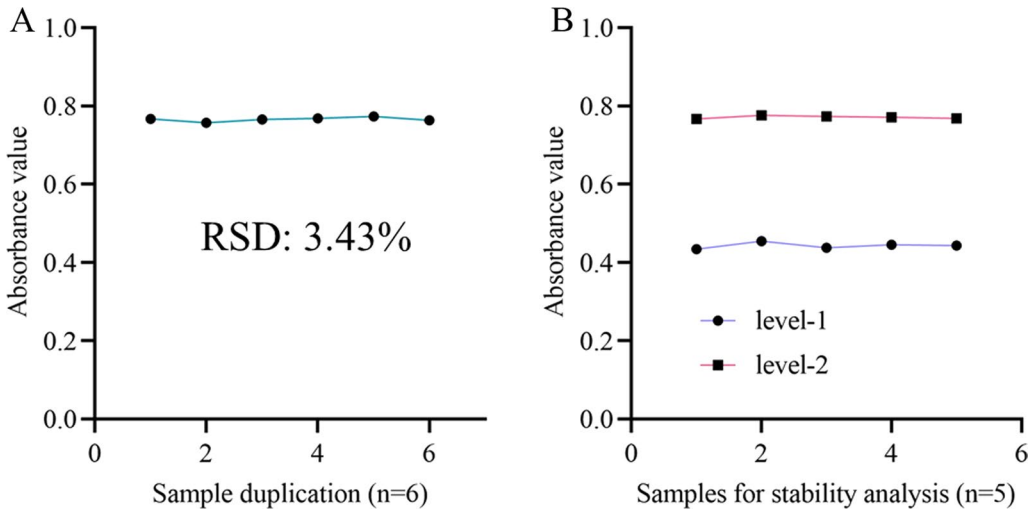

Fig. 5 Clinical application of the sensor. **A** The absorbance value of the method when detecting sample duplicates. **B** Absorbance value of the method when detecting two levels of samples

Table 1 The recovery rate of the sensor (n = 5)

Tests	Added	Report	Recovery (%)	RSD (%)
1	100	96.74	96.74	3.23
2	500	519	103.78	4.76
3	50,000	49,577	99.15	2.65

RSD relative standard deviation

biosensor that was constructed. Table 1 demonstrates that the recoveries varied between 96.74 and 103.78%, while the RSDs ranged from 2.65 to 4.76%. These results indicate that the sensor is both practical and reliable for detecting miRNA-155 in real samples.

Conclusion

To summarize, we have devised a method for detecting miRNA using EXPAR. This method effectively prevents non-specific amplification in EXPAR by using the Exo III-aided signal cycle. Compared to existing detection methods, this approach exhibits several distinct advantages, including (1) Non-specific amplification from hybridization of interfering sequences with a template in EXPAR is greatly precluded by designing a stem-loop structure in the LT probe. The binding site in the template is blocked in the stem section and could be triggered only when Exo III-based cleavages occur; (2) dual signal amplification process, including the Exo III assisted target recycling and the EXPAR process endows the method a high sensitivity for miRNA-155 detection. Based on the elegant design, the established sensor possesses a low limit of detection of 0.43 fM and shows a high selectivity to miRNA-155. In addition, this design provides a novel strategy to preclude the non-specific amplification in EXPAR. Nevertheless, the many enzymes in the reaction system are susceptible to environmental factors. Hence, the suggested approach shows significant potential as a feasible and all-encompassing framework for simultaneous analysis in clinical diagnostics and prognostics for nucleic acid detection.

Supplementary Information

The online version contains supplementary material available at https://doi.org/10.1186/s40543-024-00454-0.

Supplementary Material 1

Acknowledgements
Not applicable.

Author contributions
JD is the supervisor of the team in all research steps including data gathering, data analysis. XW and SZ, as the co-first author, has the main role for experimental data collection. All authors have read and approved the manuscript.

Funding
No funding was obtained for this study.

Availability of data and materials
All data generated or analyzed during this study are included in this published article [and its supplementary information files].

Declarations

Ethics approval and consent to participate
The manuscript does not contain clinical or trial studies on patients, humans, or animals.

Competing interests
The authors declare that they have no competing interests.

Received: 6 May 2024 Accepted: 13 June 2024
Published online: 24 June 2024

References

Bai C, Liu Y, Zhao Y, Ye Q, Zhao C, Liu Y, Wang J. Circulating exosome-derived miR-122-5p is a novel biomarker for prediction of postoperative atrial fibrillation. J Cardiovasc Transl Res. 2022;15(6):1393–405.

Chen C, Ridzon DA, Broomer AJ, Zhou Z, Lee DH, Nguyen JT, Barbisin M, Xu NL, Mahuvakar VR, Andersen MR, Lao KQ, Livak KJ, Guegler KJ. Real-time quantification of microRNAs by stem-loop RT-PCR. Nucleic Acids Res. 2005;33(20): e179.

Chen J, Zhu D, Huang T, Yang Z, Liu B, Sun M, Chen JX, Dai Z, Zou X. Isothermal Self-Primer EXPonential Amplification Reaction (SPEXPAR) for highly sensitive detection of single-stranded nucleic acids and proteins. Anal Chem. 2021;93(37):12707–13.

Emaus MN, Anderson JL. Magnetic ionic liquids as microRNA extraction solvents and additives for the exponential amplification reaction. Anal Chim Acta. 2021;1181: 338900.

Forero DA, Gonzalez-Giraldo Y, Castro-Vega LJ, Barreto GE. qPCR-based methods for expression analysis of miRNAs. Biotechniques. 2019;67(4):192–9.

Guo J, Liang Q, Zhang H, Tian M, Zhang H, Wei G, Zhang W. Exo-III enzyme-assisted triple cycle signal amplifications for sensitive and accurate identification of pathogenic bacteria. Appl Biochem Biotechnol. 2023;195(10):6203–11.

Guo H, Chen J, Feng Y, Dai Z. A simple and robust exponential amplification reaction (EXPAR)-based hairpin template (exp-Hairpin) for highly specific, sensitive, and universal microRNA detection. Anal Chem. 2024;96(6):2643–50.

He B, Zhao Z, Cai Q, Zhang Y, Zhang P, Shi S, Xie H, Peng X, Yin W, Tao Y, Wang X. miRNA-based biomarkers, therapies, and resistance in Cancer. Int J Biol Sci. 2020;16(14):2628–47.

Ho PTB, Clark IM, Le LTT. MicroRNA-based diagnosis and therapy. Int J Mol Sci. 2022;23(13):7167.

Hu W, Su H, Zeng X, Duan X, Li Y, Li L. Exo-III enzyme and DNAzyme-assisted dual signal recycles for sensitive analysis of exosomes by using personal glucose meter. Appl Biochem Biotechnol. 2023;195(2):861–70.

Hussen BM, Hidayat HJ, Salihi A, Sabir DK, Taheri M, Ghafouri-Fard S. MicroRNA: a signature for cancer progression. Biomed Pharmacother. 2021;138: 111528.

Jia H, Li Z, Liu C, Cheng Y. Ultrasensitive detection of microRNAs by exponential isothermal amplification. Angew Chem Int Ed Engl. 2010;49(32):5498–501.

Li W, Ruan KJA, Chemistry B. MicroRNA detection by microarray. Anal Bioanal Chem. 2009;394(4):1117–24.

Mishra S, Yadav T, Rani V. Exploring miRNA based approaches in cancer diagnostics and therapeutics. Crit Rev Oncol Hematol. 2016;98:12–23.

Parayath NN, Gandham SK, Amiji MM. Tumor-targeted miRNA nanomedicine for overcoming challenges in immunity and therapeutic resistance. Nanomedicine. 2022;17(19):1355–73.

Ratnasari N, Lestari P, Renovaldi D, Raditya Ningsih J, Qoriansas N, Wardana T, Hakim S, Signa Aini Gumilas N, Indrarti F, Triwikatmani C, Bayupurnama P, Setyo Heriyanto D, Astuti I, Mubarika Harjana S. Potential plasma biomarkers: miRNA-29c, miRNA-21, and miRNA-155 in clinical progression of Hepatocellular Carcinoma patients. PLoS ONE. 2022;17(2):e0263298.

Reid MS, Le XC, Zhang H. Exponential isothermal amplification of nucleic acids and assays for proteins, cells, small molecules, and enzyme activities: an EXPAR example. Angew Chem Int Ed Engl. 2018;57(37):11856–66.

Rupaimoole R, Slack FJ. MicroRNA therapeutics: towards a new era for the management of cancer and other diseases. Nat Rev Drug Discov. 2017;16(3):203–22.

Saliminejad K, Khorram Khorshid HR, Soleymani Fard S, Ghaffari SH. An overview of microRNAs: biology, functions, therapeutics, and analysis methods. J Cell Physiol. 2019;234(5):5451–65.

Takei F, Akiyama M, Murata A, Sugai A, Nakatani K, Yamashita I. RT-Hpro-PCR: a microRNA detection system using a primer with a DNA tag. ChemBioChem. 2020;21(4):477–80.

Wei H, Bu S, Wang Z, Zhou H, Li X, Wei J, He X, Wan J. Click chemistry actuated exponential amplification reaction assisted CRISPR-Cas12a for the electrochemical detection of microRNAs. ACS Omega. 2022;7(40):35515–22.

Wu Y, Fu C, Shi W, Chen J. Recent advances in catalytic hairpin assembly signal amplification-based sensing strategies for microRNA detection. Talanta. 2021;235: 122735.

Xu L, Duan J, Chen J, Ding S, Cheng W. Recent advances in rolling circle amplification-based biosensing strategies: a review. Anal Chim Acta. 2021;1148: 238187.

Yang IP, Tsai HL, Miao ZF, Huang CW, Kuo CH, Wu JY, Wang WM, Juo SH, Wang JY. Development of a deregulating microRNA panel for the detection of early relapse in postoperative colorectal cancer patients. J Transl Med. 2016;14(1):108.

Zhao W, Ali MM, Brook MA, Li Y. Rolling circle amplification: applications in nanotechnology and biodetection with functional nucleic acids. Angew Chem Int Ed Engl. 2008;47(34):6330–7.

Zhao L, Mao J, Hu L, Zhang S, Yang X. Self-replicating catalyzed hairpin assembly for rapid aflatoxin B1 detection. Anal Methods. 2021;13(2):222–6.

Publisher's Note